12^{th} International Conference on Fracture Mechanics of Concrete and Concrete Structures
FraMCoS-12
B.L.A. Pichler, Ch. Hellmich, P. Preinstorfer (Eds)

https://doi.org/10.21012/FC12.1359
MS13-1:1

COMPUTATIONAL AND ANALYTICAL MODELLING OF CARBONATION-INDUCED SPALLING OF THE CONCRETE COVER

ANDREAS DEKEYSER*, ELS VERSTRYNGE†, ROMAN WAN-WENDNER*, WOUTER BOTTE* AND ROBBY CASPEELE*

* Ghent University, Department of Structural Engineering and Building Materials
Technologiepark-Zwijnaarde 60, 9052 Ghent, Belgium
†KU Leuven, Department of Civil Engineering
Kasteelpark Arenberg 40 - box 2448, 3001 Leuven, Belgium
e-mail: anddkeys.dekeyser@ugent.be

Key words: Uniform Corrosion, Carbonation, Cover Spalling, Numerical Modelling

Abstract. Concrete is one of the most abundantly used materials in the building industry and corrosion of the reinforcement steel is one of the main reasons of degradation in concrete structures. Corrosion of the rebars not only reduces the steel cross-section, it is also accompanied by a volume increase due to the formation of rust products, resulting in rising internal expansion stresses on the concrete. Eventually, cracks may form when the tensile stress reaches the tensile strength of concrete, and further propagation of these cracks towards adjacent rebars or to the surface may lead, respectively, to delamination and spalling of the concrete cover. In this work, spalling behaviour due to a uniform radial pressure, relevant for carbonation-induced corrosion, is analysed using a 2D Finite Element model. This numerical model is used to assess the adequacy of existing analytical models in literature predicting the peak pressure during spalling. The allowable peak pressure can be seen as a resistance against spalling, which may be related to the corrosion level and hence is relevant in relation to the reliability-based assessment of degrading structures.

1 INTRODUCTION

Ageing of civil structures is a common problem in the construction industry, which goes hand in hand with the development of renovation and refurbishment plans. Assessing and managing degrading structures, however, require a certain understanding of the physical phenomena. One of the main reasons of degradation of concrete structures is corrosion of reinforcement steel [3], which is accompanied by a reduction of the steel cross-section, and a volume increase due to the formation of rust products. The latter may result in internal expansion stresses in the concrete, which may eventually lead to cracking, delamination and spalling of the concrete cover. Spalling of the concrete cover may endanger passers-by, reduces the structural cross-section of the element and reduces the remaining service life due to its influence on the corrosion process. Yet, limited models are available that can predict this behaviour, and are suitable to assess this failure mode of degrading concrete structures.

This work considers a FE model to explicitly simulate crack propagation to analyse spalling behaviour induced by a uniform internal radial pressure. This model will be used to assess the adequacy of two existing models in literature which predict the peak pressure occurring during spalling of the concrete cover. This peak pressure is a measure of the resistance against spalling and hence is relevant in relation

to the reliability-based assessment of degrading concrete structures. First, the existing analytical models describing spalling of the concrete cover are briefly discussed. Further, the structure of the FE model is explained, including a validation using test results from literature. Subsequently, the numerical model is used to assess the adequacy of the existing analytical models. Finally, the conclusions of this work are given.

2 STATE OF THE ART

Currently, models exist predicting corrosion-induced concrete cover cracking using thick-walled cylinder models to relate the deformation induced by the expanding corroding rebar with the internal pressure [4–11]. Only a limited amount of models exist that describe corrosion-induced spalling of the concrete cover. One way to approach the phenomenon, is by applying a uniform internal pressure at the internal surface of the opening representing the reinforcement steel instead of an expanding corroding rebar by using for example a hydraulic inflator device [1,2,12]. Such tests can measure the maximum occurring internal pressure during loading, representing a measure of the resistance against spalling. After reaching this peak pressure, a softening branch develops until the concrete cover spalls [2]. As an example of this softening behaviour, in Figure 1, the pressure, p, is plotted in function of the out-of-plane displacement of the surface, u_y, c_y is the concrete cover thickness, and ϕ_0 is the rebar diameter.

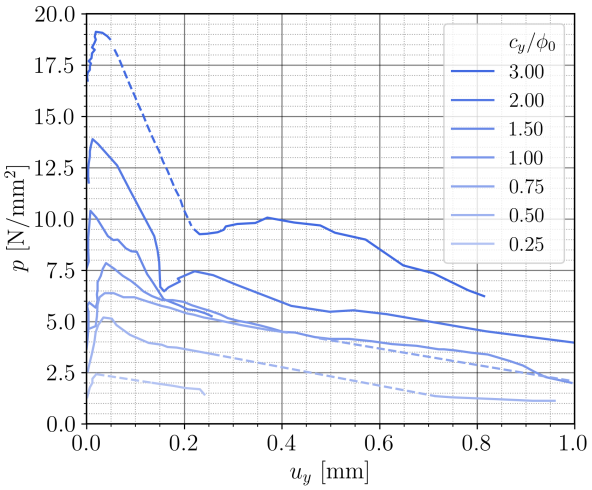

Figure 1: Internally applied pressure as a function of the out-of-plane displacements of the surface for a varying concrete cover thickness where the dashed lines correspond with missing data, adapted from Moccia et al. [2].

Williamson and Clark [1] made an attempt on predicting the peak pressure by applying the kinematic theorem on the spalled concrete cover assuming that the system obtains a translational motion, visualized in Figure 2a. However, many effectiveness factors had to be used

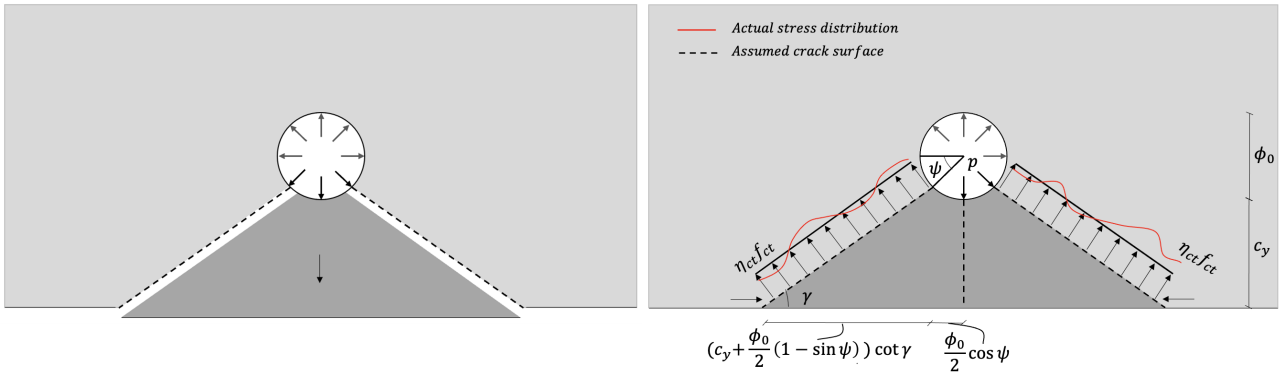

(a) **(b)**

Figure 2: Modes for the prediction of the peak pressure: (a) assumed translational motion applied in the kinematic theorem in the model of Williamson and Clark [1], and (b) assumed failure plane with corresponding stress distributions in the model of Moccia et al. [2].

since an upper-bound theorem was applied, indicating that possibly another method would be more effective.

Subsequently, Moccia et al. [2] developed a model predicting the peak pressure, by applying the static theorem, starting from a certain assumed failure plane, visualized in Figure 2b, where ψ is a variable and γ is taken as a constant value equal to 37°. It should be mentioned that experiments have shown that this angle can range from 30° to 45° in case of non-uniform corrosion [14]. Furthermore, Moccia et al. [2] assume an averaged tensile strength, $\eta_{ct} f_{ct}$ with $\eta_{ct} = 0.80$, along the cracks. By stating that the vertical equilibrium needs to be satisfied, the pressure can be written in terms of the variable ψ. Applying limit analysis, the expression of p can be minimized with respect to ψ, such that the peak pressure, or also called the critical pressure, yields [2]:

$$p_{cr} = 2\frac{\eta_{is}\eta_{ct} f_{ct}}{\tan\gamma}\sqrt{\frac{c_y}{\phi_0} + \left(\frac{c_y}{\phi_0}\right)^2}\left(\frac{d_{dg}\phi_{ref}}{d_{dg,ref}\phi_0}\right)^{\frac{1}{m}} \quad (1)$$

in which $\eta_{is} = 0.6$ is a reduction factor to account for the bleeding effect on the tensile strength of concrete in case the rebar is a top rebar. If the rebar is a bottom rebar, then $\eta_{is} = 1$, which will be considered in this work. Furthermore, the factor $\left(\frac{d_{dg}\phi_{ref}}{d_{dg,ref}\phi_0}\right)^{\frac{1}{m}}$ takes the size effect into account as larger openings are accompanied by smaller peak stresses [2], where the reference values equal $\phi_{ref} = 20$ mm, $d_{dg,ref} = 32$ mm, $m = 3$, and an average roughness [2]:

$$d_{dg} = \min\{40\text{ mm}; 16{+}d_g\} \quad (2)$$

for $f_c \leq 60$ N/mm^2, and d_g the maximum aggregate size. It should be mentioned that Moccia et al. [2] extended this model in case multiple rebars are present in the failure plane and also in case spalling of the concrete cover is caused by pull-out failure. However, these cases will not be treated in this paper.

Another model developed by Su and Zhang [19] gives a relation between the corrosion degree of non-uniform corrosion, the crack width, and the amount of bulging of the surface assuming that the concrete behaves rigid in the direction perpendicular to the surface and that the spalling concrete cover obtains purely a rotational motion. At first, concrete behaves linear elastic after which a crack develops when the tensile stress reaches the tensile strength of concrete. This way, the crack width or the corrosion degree can be estimated by measuring the amount of bulging of the concrete surface. Although it does not have a direct link with the models predicting the peak pressure when an internal uniform pressure is applied, it gives insight into the kinematics of the system.

3 FINITE ELEMENT MODEL

A FE model is developed to analyse spalling behaviour induced by a uniform radial pressure using Abaqus FEA software. A 2D rectangular section with size 400 x 250 mm is modelled in which the shape of a rebar is cut out as a hole and placed in the centre line of the width. In order not to excessively increase the computational time, three-node triangular plane stress elements are used. Triangular elements allow to model more complex shapes, resulting in a crack path which is less mesh-dependent. Furthermore, a plane stress situation is consistent with the assumption underlying the classical thick-walled cylinder model used for the prediction of cover cracking [4–11]. The aggregates are not modelled. However, previous mesoscale models in which the aggregates are explicitly modelled as randomly distributed through the mortar matrix have shown that cracks tend to propagate along the aggregates [20, 21]. Not modelling the aggregates is consistent with the analytical models discussed in section 2 where straight crack paths are assumed. An approximate mesh size of 1 mm is implemented in the critical zones, i.e. in the vicinity of the rebar. Going further away from the rebar, the mesh size is increased to reduce the computational time. The model is load-controlled by incrementally increasing the uniform radial pressure on the internal surface in time. The explicit time integration scheme is used in order

to prevent convergence problems when modelling crack propagation in concrete. As such, it was ensured that the kinetic energy is negligible compared to the internal energy of the system.

3.1 Constitutive law of concrete

To properly model crack propagation in concrete, the damage-plasticity theory as described in Lubliner et al. [22] and later modified by Lee and Fenves [23], is applied in the FE model. It assumes that concrete mainly fails in tension as cracking and in compression as crushing [20]. The model is suitable to predict non-linear behaviour for both dynamic and static loading. It accounts for the stiffness degradation for plastic straining in compression and tension, and it accounts for the triaxial effect [20]. In this work, it is assumed that concrete behaves linear elastic in tension and compression until the tensile stress reaches the tensile strength of concrete [16], and the compressive stress reaches $\sigma_c = 0.4 f_{cm}$ [15] respectively. After reaching this point, the following equations are used for concrete in tension and compression respectively [15, 16]:

$$\frac{\sigma_c}{f_{cm}} = -\left(\frac{k\eta - \eta^2}{1 + (k-2)\eta}\right) \tag{3}$$

$$\sigma_{ct} = \begin{cases} f_{ctm}\left(1 - 0.8\frac{w}{w_1}\right), & w \leq w_1 \\ f_{ctm}\left(0.25 - 0.05\frac{w}{w_1}\right), & w_1 < w \leq w_c \end{cases} \tag{4}$$

in which $\eta = \varepsilon_c/\varepsilon_{c1}$, $k = 1.05 E_{cm}|\varepsilon_{c1}|/f_{cm}$, ε_{c1} is the strain at maximum compressive stress (Table 1), $\varepsilon_{c,lim}$ is the nominal ultimate strain (Table 1), f_{cm} is the mean compressive strength, w is the crack width, $w_1 = G_f/f_{ctm}$, $w_c = 5G_f/f_{ctm}$ is the crack width for which the tensile stress equals zero, $G_f = 73 f_{cm}^{0.18}$ is the fracture energy, and f_{cm} is the mean tensile strength. So the post-fracture constitutive law for concrete in tension is modelled using a fracture mechanics approach in which the residual tensile stress is expressed in function of the crack width using a bilinear curve.

The damage parameter, defining the magnitude of the stiffness reduction, is defined using the stress state for compressive and tensile stress respectively [17]:

$$d_c = 1 - \frac{\sigma_c}{\sigma_{cu}} \tag{5}$$

$$d_t = 1 - \frac{\sigma_{ct}}{\sigma_{ctu}} \tag{6}$$

in which σ_{cu} and σ_{ctu} are respectively the ultimate compressive and tensile stress, i.e. the mean compressive and tensile strength. The stiffness reduction is then formulated as $(1 - d_i)E_{cm}$, with $i = c, t$ [17].

The plasticity parameters are taken as the default values, Table 1. The dilation angle typically ranges between 30°-40° [18], for which a higher dilation angle corresponds with a higher ductility [17]. Here, the angle was chosen equal to $40°$ as this showed to have good correspondence compared with the test results of Moccia et al. [2].

3.2 Validation of the numerical model

To validate the numerical model, the test results of Moccia et al. [2] are used. The relevant

Table 1: Strains ε_{c1} and $\varepsilon_{c,lim}$ for a concrete with a grade up until C50 [15, 16], and the plasticity parameters for the damage-plasticity model [17, 18].

Concrete grade	C12	C16	C20	C25	C30	C35	C40	C45	C50
ε_{c1} [‰]	-1.9	-2.0	-2.1	-2.2	-2.3	-2.3	-2.4	-2.5	-2.6
$\varepsilon_{c,lim}$ [‰]	-3.5	-3.5	-3.5	-3.5	-3.5	-3.5	-3.5	-3.5	-3.4

Dilation angle [°]	Eccentricity [-]	$fb0/fc0$ [-]	K [-]	Viscosity parameter [-]
40	0.1	1.16	2/3	0

material properties are mentioned in Table 3, CM11 is the test series with a varying concrete cover, and CM12 is the test series with a varying rebar diameter. The modulus of elasticity is estimated using the following equation [15]:

$$E_{cm} = 22000 \left(\frac{f_{cm}}{10} \right)^{0.3} \tag{7}$$

Table 3: Material properties applicable to the tests of Moccia et al. [2].

Series	f_c [N/mm^2]	f_{ct} [N/mm^2]
CM11	39.7	2.49
CM12	40.5	2.78

To compare the numerical results with the test results in Moccia et al. [2], it is of utmost importance to have an understanding of the difference between the executed tests and the numerical model. In the testing campaign of Moccia et al. [2], hydraulic inflator devices were used to induce a radial pressure on the inner surface, for which the inflator membrane has a negligible stiffness. The pressure was measured by means of a pressure gauge. As is clear from Figure 1, softening behaviour is captured, indicating that a pressure release between the inflator device and the spalling concrete body is included. A load-controlled model in ABAQUS, however, is not able to capture this post-peak softening behaviour correctly, as will be discussed in the following.

Looking at the numerical model, the applied pressure is incrementally increased as a result of the load control application. However, when cracks appear in the first row of elements around the rebar circumference, the transferred pressure to the system depends on the amount of stiffness degradation of these elements as a result of the damage-plasticity theory applied in this model. The principal compression stress around the rebar circumference is shown in Figure 3, where the bottom, i.e. at $\theta = 180°$, is the side located near the concrete surface. The effect of cracked elements is clearly visible at the locations where the principal compression stress obtains a lower value.

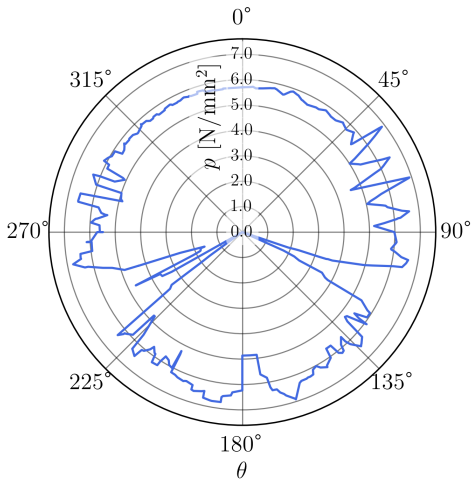

Figure 3: Principal compression stress at $p = 6.12$ N/mm^2 measured at the first row of elements around the rebar circumference, $c_y = 15$ mm for CM11.

Taking this into account, the evolution of the average principal compression stress, p_{avg}, during loading can be plotted as a function of the maximum out-of-plane displacement of the sur-

Table 2: Comparison of the maximum pressures between the measured values reported in Moccia et al. [2] and the estimated numerical values for the different test series.

Series	ϕ_0 [mm]	c_y/ϕ_0 [-]	$p_{cr,measured}$ [N/mm^2] [2]	$p_{cr,numerical}$ [N/mm^2]
CM11	20	0.50	5.2	5.9
	20	0.75	6.4	6.7
	20	1	7.8	8.4
CM12	10	1.25	11.4	12.2
	28	1.25	10.8	10.9

face, see Figure 4.

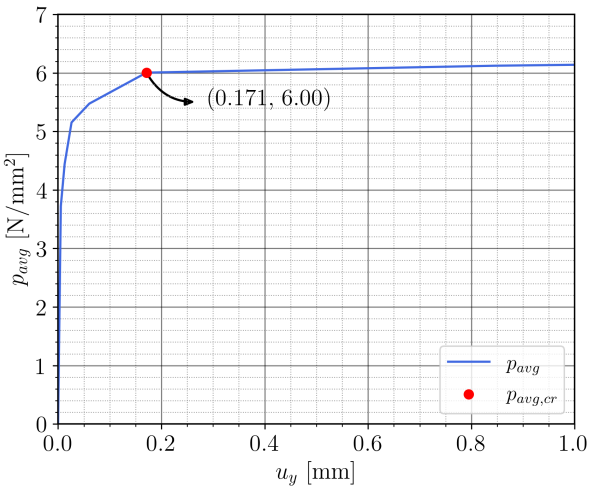

Figure 4: Average principal compression stress along the first row of finite elements at the rebar circumference as a function of the maximum out-of-plane displacement of the surface, c_y = 15 mm, $c_y/\phi_0 = 0.75$ for CM11.

It can be seen that the post-peak behaviour is not captured accurately compared to what is expected (see Figure 1). This is the result of the application of a load-controlled model. In an incremental implicit integration scheme, the arc length method could be applied to capture this post-peak softening branch. However, due to the application of concrete damage-plasticity theory applied as constitutive law, full propagation of cracks through the cover results in large displacements and could lead to convergence issues. Another solution for capturing the post-peak behaviour more accurately is a displacement controlled method by incrementally increasing the magnitude of a uniform radial displacement field, which still would allow to use the explicit integration scheme to tackle convergence issues. Yet, an equivalent response compared to when a uniform radial pressure is applied can not be ensured, especially when cracks form, resulting in a non-linear response. Nevertheless, the domain of loading which is of interest for this analysis is until reaching the predicted peak pressure, i.e. before the system obtains large deformations for which softening behaviour is expected. The moment the average pressure stagnates, i.e. at $p_{avg,cr}$ = 6 N/mm^2, is used to predict the peak pressure which is applied in the corresponding load step on the inner surface, which is p_{cr} = 6.7 N/mm^2 in this case. This calculation can be done for several geometrical configurations of the test series CM11 and CM12. The results are presented in Table 2. The critical pressures are systematically overpredicted by the numerical model compared to the tested values. However, the numerical model still accurately captures the peak pressures. The overprediction can be attributed to the differences between the tested pressure, where at reaching p_{cr} already some minor softening behaviour is captured, and the numerical model, where this softening behaviour is not included. Additionally, the three-node triangular elements predict spurious shear strains, leading to an overestimation of the stiffness [13].

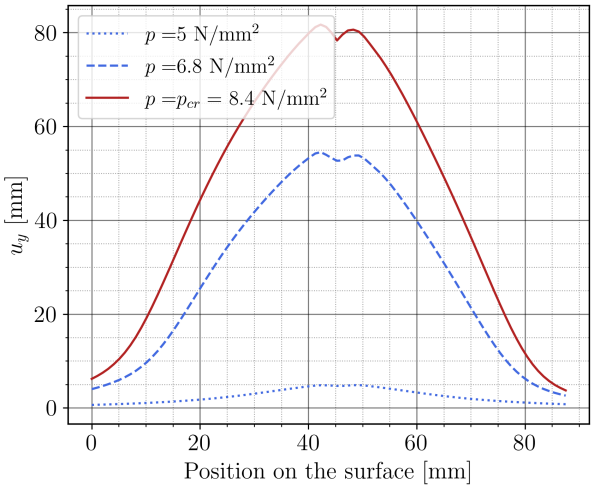

Figure 5: Out-of-plane displacement of the surface captured by the FE model for different load steps for c_y = 20 mm and test series CM11, measured between the locations where the inclined cracks meet the surface.

4 RESULTS AND DISCUSSION

In the following, the FE model is used to analyse spalling behaviour. Furthermore, these results are used to assess the adequacy of the underlying assumption of (1) the model of Williamson and Clark [1], where a translational

motion was assumed for the spalled concrete body in the kinematic method to predict the peak pressure, and (2) the assumed stress distribution for the static method in the model of Moccia et al. [2].

4.1 Analysis of the kinematics of the system

The system's kinematics can be analysed using the FE model as developed in section 3, by plotting the out-of-plane displacements of the surface, see Figure 5. The vertical displacements decrease approximately linearly going further away from the rebar, when moving away from the centre line. This indicates that rather a rotational displacement field develops. Since the kinematic theorem is an upper-bound theorem, the predicted critical pressure will indeed be an overestimation if some assumptions do differ significantly with reality, introducing the need for correction factors.

4.2 Analysis of the crack pattern and corresponding stress distributions

In Figure 6, the simulated crack pattern is compared with the tested crack pattern in Moccia et al. [2], for $\phi_0 = 20$ mm, $c_y = 20$ mm

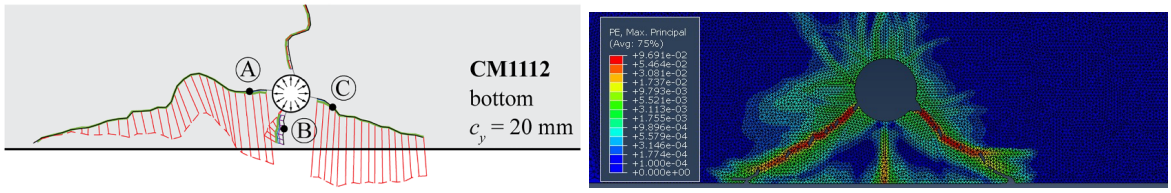

(a) **(b)**

Figure 6: (a) Tested crack pattern [2], and (b) simulated crack pattern, for $\phi_0 = 20$ mm, $c_y = 20$ mm, and test series CM11.

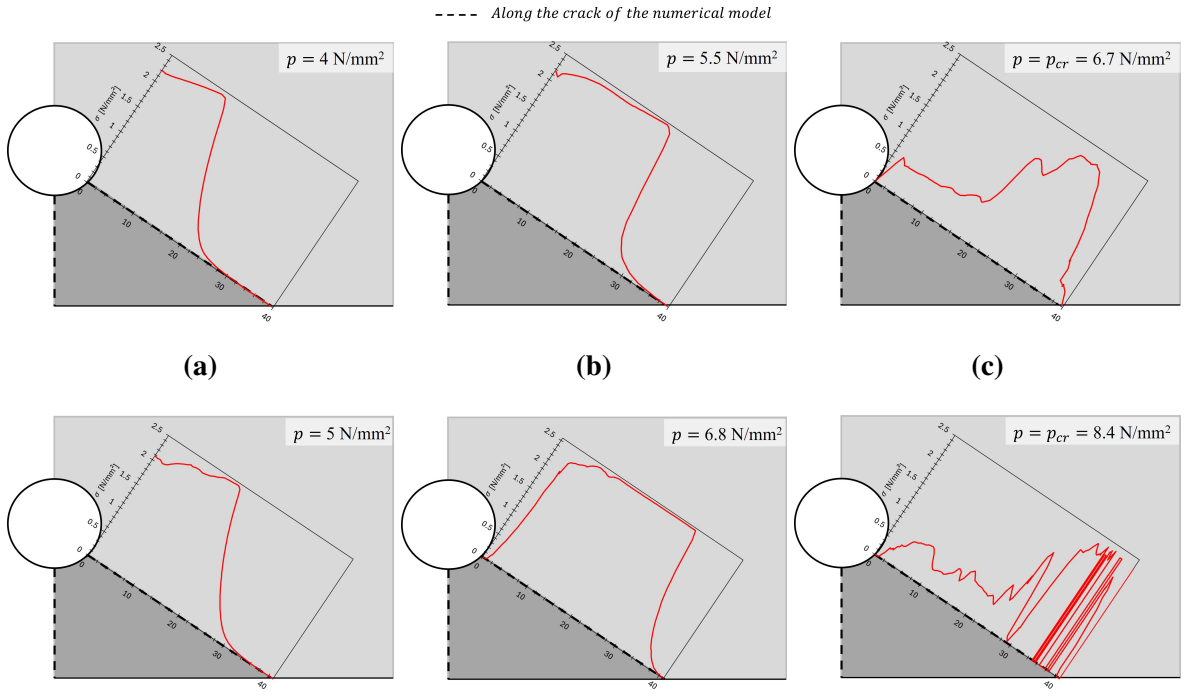

(a) **(b)** **(c)**

(d) **(e)** **(f)**

Figure 7: Principal tensile stress distribution evolution along the inclined crack for the properties of test series CM11 and (a-c) $c_y = 15$ mm, and (d-f) $c_y = 20$ mm.

and test series CM11. Considering that the aggregates were not explicitly modelled, the simulated crack pattern corresponds reasonably well with the tested crack pattern. Furthermore, it is also consistent with the assumed failure plane in the analytical model of Moccia et al. [2], see Figure 2b.

The evolution of the principal tensile stress distribution along the inclined crack for subsequent load steps until reaching p_{cr} is plotted in Figure 7 in case $c_y = 15$ mm and $c_y = 20$ mm respectively. First, case $c_y = 15$ mm will be discussed. In Figure 7a, the crack has partly propagated through the concrete, where the tip of the crack corresponds with the principal stress being equal to the tensile strength of concrete, the reduction of the principal tensile stress going from the crack tip towards the rebar indicates a certain widening of the crack considering fracture mechanics. Increasing the internal pressure, Figure 7b and later Figure 7c, it is observed that the inclined crack propagates further towards the surface. In Figure 7c, a significant stress reduction has occurred for the part between the rebar and the stress peak, indicating a significant widening of the crack. The same observations can be made looking at the principal tensile stress distribution evolution along the inclined crack in case $c_y = 20$ mm.

The final steps, Figure 7c and 7f, correspond with an internal pressure equal to the predicted critical pressure. At this stage, the stress distributions have an irregular shape, which are decisive for the prediction of the critical pressure in the static theorem as applied in the model of Moccia et al. [2]. In this analytical model, the stress was taken as uniform and equal to an averaged tensile strength, $\eta_{ct} f_{ct}$, along the inclined crack, see Figure 2b. For engineering purposes, having a measure of the resistance against spalling using a simplified approach is preferred, as demonstrated in the prediction of p_{cr} using a uniform distribution in the model of Moccia et al. [2]. However, the implementation of the factor η_{ct} in Moccia et al. [2], where it is referred to as an averaged tensile strength, can be questioned. For a correct estimation of the critical pressure according to the static theorem, it is important that the stress distributions are resembling a realistic situation. In this context, an averaged stress along the inclined crack at the moment $p = p_{cr}$, eventually resulting in a uniform distribution, to determine the factor η_{ct} would be more suitable.

5 Conclusions

This paper analysed spalling behaviour using a FE model in case a uniform radial pressure is applied at the surface representing the rebar circumference. The damage-plasticity theory was used to model concrete, which allowed to study crack propagation with corresponding stress distribution evolutions. The numerical model was used to compare with the assumptions underlying two models predicting the peak pressure during spalling, i.e. the model of Williamson and Clark [1] and Moccia et al. [2], from which the following can be concluded:

- The analysis of the kinematics of the spalling body revealed a more dominant rotational motion, indicating that the latter would be more appropriate to apply in the kinematic theorem.

- The principal tensile stress distribution along the inclined crack was analysed at the moment that the internal pressure equals the peak pressure. This stress distribution exhibited an irregular shape, indicating that it would be more suitable that the factor η_{ct} is determined by averaging the principal tensile stress distribution along the inclined crack at the moment $p = p_{cr}$.

REFERENCES

[1] Williamson, S. J., and Clark, L. A. 2000. Pressure required to cause cover cracking of concrete due to reinforcement corrosion. *Magazine of Concrete Research*, 52, 455–467.

[2] Moccia, F., Fernández Ruiz, M., and Muttoni, A. 2021. Spalling of concrete cover

induced by reinforcement. *Engineering Structures*, 237, 112188.

[3] Portland Cement Association (PCA) 2002. Types and causes of concrete deterioration. *Portland Cement Association*.

[4] Bažant, Z. P. 1979. Physical model for steel corrosion in concrete sea structures—application. *Journal of the Structural Division*, 105(6), 1155–1166.

[5] Balafas, I., and Burgoyne, C. J. 2011. Modeling the structural effects of rust in concrete cover. *Journal of Engineering Mechanics*, 137(3), 175–185.

[6] Bhargava, K., Ghosh, A. K., Mori, Y., and Ramanujam, S. 2005. Modeling of time to corrosion-induced cover cracking in reinforced concrete structures. *Cement and Concrete Research*, 35(11), 2203–2218.

[7] Chernin, L., and Volokh, K. Y. Val, D. V. 2010. Analytical modelling of concrete cover cracking caused by corrosion of reinforcement. *Materials and Structures*, 43(4), 543–556.

[8] El Maaddawy, T., and Soudki, K. 2007. A model for prediction of time from corrosion initiation to corrosion cracking. *Cement and Concrete Composites*, 29(3), 168–175.

[9] Pantazopoulou, S., and Papoulia, K. (2001). Modeling cover cracking due to reinforcement corrosion in RC structures. *Journal of Engineering Mechanics*, 127(4), 342-351.

[10] Wang, X.-H., and Liu, X. 2004. Modelling effects of corrosion on cover cracking and bond in reinforced concrete. *Magazine of Concrete Research*, 56, 191–199.

[11] Wang, X.-H., and Liu, X. 2004. Modeling bond strength of corroded reinforcement without stirrups. *Cement and Concrete Research*, 34(8), 1331–1339.

[12] Morinaga, S. 1988. Prediction of service lives of reinforced concrete buildings based on the rate of corrosion. Technical Report 23, Institute of Technology, Shimizu Corporation.

[13] Muftu, S. 2022. Rectangular and triangular elements for two-dimensional elastic solids. Chapter 8 in *Finite Element Method*, edited by Sinan Muftu, 257–291. Academic Press.

[14] Qiao, D., Nakamura, H., Yamamoto, Y., and Miura, T. 2016. Crack patterns of concrete with a single rebar subjected to non-uniform and localized corrosion. *Construction and Building Materials*, 116, 366–377.

[15] European Committee for Standardization. 2005. NBN EN 1992-1-1: Eurocode 2 - Design of concrete structures - Part 1.1: General rules and rules for buildings, bridges, and civil engineering structures.

[16] Fédération internationale du béton (fib). 2012. fib Bulletin No. 65: Model Code 2010 - Final draft, Volume 1.

[17] Hafezolghorani Esfahani, M., Hejazi, F., Vaghei, R., Bin Jaafar, M. S., and Karimzade, K. 2017. Simplified damage plasticity model for concrete. *Structural Engineering International*, 27(1), 68–78.

[18] Thanh Cuong, L., Le Minh, H., and To, T. S. 2022. A nonlinear concrete damaged plasticity model for simulation reinforced concrete structures using Abaqus. *Frattura ed Integrità Strutturale*, 59, 232–242.

[19] Su, R. K. L., and Zhang, Y. 2019. A novel elastic-body-rotation model for concrete cover spalling caused by non-uniform corrosion of reinforcement. *Construction and Building Materials*, 213, 549–560.

[20] Du, X., Jin, L., and Zhang, R. 2014. Modeling the cracking of cover concrete due to

non-uniform corrosion of reinforcement. *Corrosion Science*, 89, 189–202.

[21] Zhang, X., Zhang, Y., Liu, B., Liu, B., Wu, W., and Yang, C. 2021. Corrosion-induced spalling of concrete cover and its effects on shear strength of RC beams. *Engineering Failure Analysis*, 127, 105538.

[22] Lubliner, J., Oliver, J., Oller, S., and Oñate, E. 1989. A plastic-damage model for concrete. *International Journal of Solids and Structures*, 25(3), 299–326.

[23] Lee, J., and Fenves, G. L. 1998. Plastic-damage model for cyclic loading of concrete structures. *Journal of Engineering Mechanics*, 124(8), 892–900.